Size-dependent behaviors of femtosecond laser-prototyped polymer micronanowires

Kenji Takada,[1] Dong Wu,[2] Qi-Dai Chen,[2] Satoru Shoji,[1] Hong Xia,[2] Satoshi Kawata,[1] and Hong-Bo Sun[2,*]

[1]*Department of Applied Physics, Osaka University, Suita, Osaka 565-0876, Japan*
[2]*State Key Laboratory on Integrated Optoelectronics, College of Electronic Science and Engineering, Jilin University, 2699 Qianjin Street, Changchun 130012, China*
[*]*Corresponding author: hbsun@jlu.edu.cn*

Received November 4, 2008; revised January 8, 2009; accepted January 15, 2009; posted January 23, 2009 (Doc. ID 103598); published February 19, 2009

A remarkable recent progress in two-photon photopolymerization is the achievement of fabrication resolution around tens of nanometers, establishing a femtosecond laser as a nanofabrication tool. However, how the superresolution has been made possible is still under arguement. We propose a concept of polymer network permeability to solvents, meaning a structure-loosened nanopolymer state that allows free penetration of small molecules to interpret the mechanism. Experimentally, we found proof showing existence of the state, including an unusually large volume shrinkage rate (>60%), shape-memory effect, a giant softness of nanospring, and the mechanical stability of rinsed two-photon written polymer nanowires. © 2009 Optical Society of America

OCIS codes: 220.4000, 220.4241, 160.5470, 120.4610, 110.4235, 130.3120.

Femtosecond laser micronanoprototyping of photopolymerizable resins has been proved a powerful approach for the fabrication of three-dimensional (3D) structures with a nanoscale feature size [1–13]. Application examples range from integrated optical components [3–6] to functional micronanomechanical parts [7–9]. The recent breakthrough of fabrication spatial resolution [14], ~20 nm in single-fiber formation [15] and ~10 nm in device shape definition [5], is particularly notable. It makes pinpoint two-photon polymerization a convincing nanotechnique. However, questions remaining to be answered include, what are the determining factors responsible for "superresolution?" What characteristics appear when the polymer size enters the nanoregime? These issues are essential for both structures and functions of micronanodevices to be quantitatively designed. In this Letter, we designed and fabricated by two-photon photopolymerization a series of polymer micronanowires, either suspended or affixed to substrate. Comparative studies allow us to reach the conclusion that achievement of the superresolution is closely related to a loosened polymer network status that permits free removal and penetration of small molecules, what we call polymer network permeability to solvents.

Figure 1 shows the scanning electron microscopic (SEM) image of array of wires that were laser written from a urethane acrylate resin, SCR 500 (JSR). Experimentally, laser pulses of 780 nm in wavelength, 130 fs half width at an 82 MHz repetition rate first underwent beam expansion and then were delivered to and focused by a high-NA (1.4) objective lens. A galvano mirror pair scans the laser focal spot point by point with a 50 nm step in the lateral dimensions, which is sufficient to guarantee the smoothness and the continuity of wires [16]. The wires are suspended between two 2.0-μm-high polymerized anchors with their longitudinal axis 1.5 μm above the glass substrate. Each wire consists of three segments of varied diameters, thicker at the sides and thinner at the central portion. The lateral widths [Fig. 1(a)] of the side and central portions are 210 and 65 nm and in the vertical direction [Fig. 1(b)], 650 and 190 nm, respectively. Reduction of exposure intensity thin wires, for example, a wire of 25 nm width is shown in the lower inset of Fig. 1(a).

The lateral size of the wires is far smaller than the diffraction limit [13,16]. It is generally considered

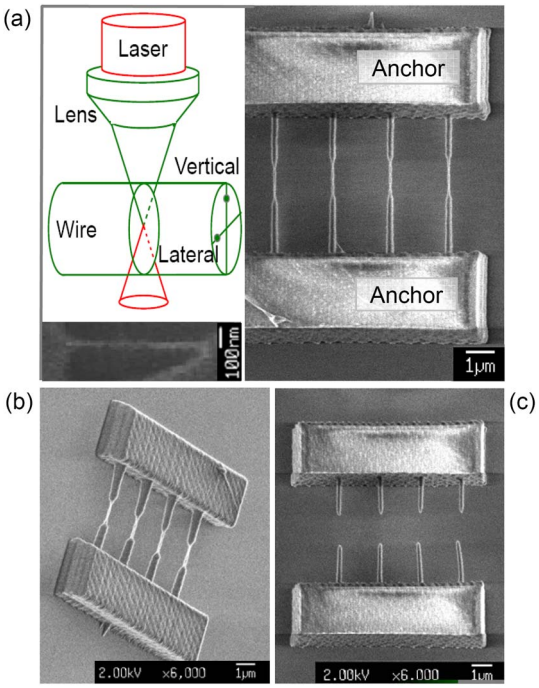

Fig. 1. (Color online) Suspended array of wires. (a) SEM images. The exposure duration of the ended and the central segments are, under a laser pulse energy of 75 pJ at the focal spot, 8 and 2 ms, respectively. The left inset illustrates the fiber dimensions related to the focused laser beam. (b) Tilted view of the entire construction. (c) Array of wires under weaker exposure, i.e., the exposure duration is 1 ms.

that the thresholding effect owing to the radical quenching is the major factor [13,16]. Is that all? What more of a role is a material playing? Low exposure inevitably leads to a low density of cross-linking of polymer chains. Upon rinsing, an essential step of fabrication, small molecules, such as partly polymerized monomer pieces, can be removed from the interchain intervals, leaving a loosened polymer network. This is the status we called polymer network permeability to solvents. It is experimentally found that the smallest wire diameters achieved with different types of resins are approximately 30 nm for NOA 61 and 45 nm for SU-8, which was found almost independent of the solvent species but possibly related to the molecular structure of materials. For SCR 500 resin, it took approximately 2 min by acetone and 5 min by ethanol, respectively, to reach the 25 nm diameter limit [Fig. 2(a)]. The faster resolving may be due to the existence of carbonyl in both urethane acrylate and acetone and closer polarity between urethane acrylate and acetone than between urethane acrylate and ethanol.

A series of experiments were designed to testify the permeability model. Suspended wires of different diameters were produced [Fig. 2(b) and the lower inset of Fig. 2(d)]. As a reference, wires with the same original shapes and sizes as those in Fig. 2(a) are drawn on a cover glass [Fig. 2(c) and the upper inset of Fig. 2(d)]. The reference wires, half truncated below their axis level and tightly adhered to the substrate surface, are subjected to insignificant deformation, preserving the designed size and shape. For the purpose of quantitative comparison, a linear shrinkage rate, α, is defined by the ratio of the lateral sizes of suspended (δ_S) and reference (δ_R) wires as $\alpha = (\delta_R - \delta_S)/\delta_R$. When the lateral diameter decreases, α rapidly increases from 2.5% at 450 nm to around 35% at $\delta_R \sim 200$ nm, where the significant size-dependent shrinkage tends to saturate [Fig. 2(c)]. It is understandable as follows: upon rinsing commencing, the wire is being attacked by solvent molecules gradually from the surface to its internal portion, expelling encapsulated small molecular pieces out of the network of chains. When the entire wire volume is cleaned, the polymer network becomes permeable, staying relatively stable, and the shrinkage rate of the wires is no longer sensitively affected by the extension of the rinsing duration.

Note that so far we consider only the lateral shrinkage. It is reasonable to assume that the same rate of shrinkage occurs along the vertical direction in a suspended wire. This gives rise to a cross-sectional shrinkage rate of 58%. The longitudinal axis, as the largest dimension of the wires, should have the greatest amount of shrinkage if their ends are not fixed. An alternative experimental scheme was therefore designed to evaluate the shrinkage along this direction. Suspended arrays of bent wires with radius r, open angle θ, and lateral thickness δ_S [Figs. 3(a) and 3(c)] were prepared. The reference wires of the same sizes and shapes [Fig. 3(b)] adhered to a glass substrate experienced no detectable shape deformation after being rinsed and dried. In contrast, all suspended wires are straightened, for

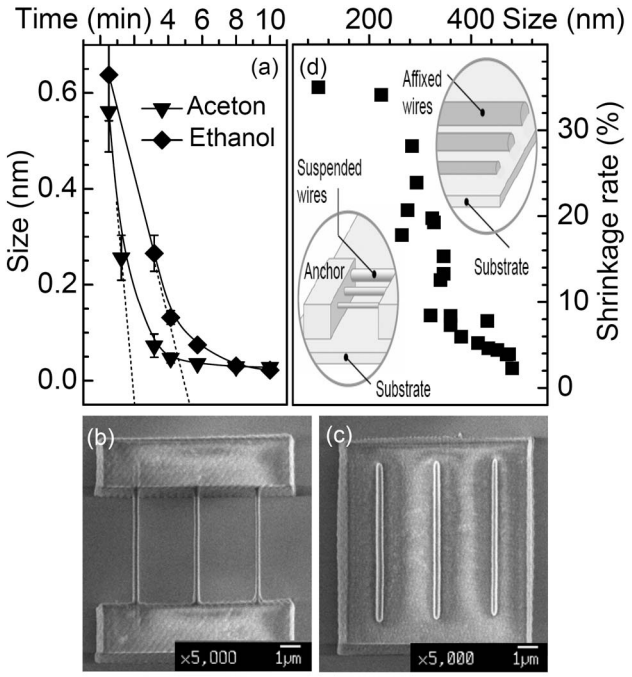

Fig. 2. Size-dependent polymer shrinkage: (a) size of wires produced under conditions described in Fig. 1 versus rinsing time by different solvents; (b) SEM images of suspended wires of varied laterals size; (c) reference wires with the same sizes and shapes as in (b), which are affixed to a glass substrate; (d) shrinkage rate dependent on the lateral sizes of wires. The lateral axis is the size of the reference wires.

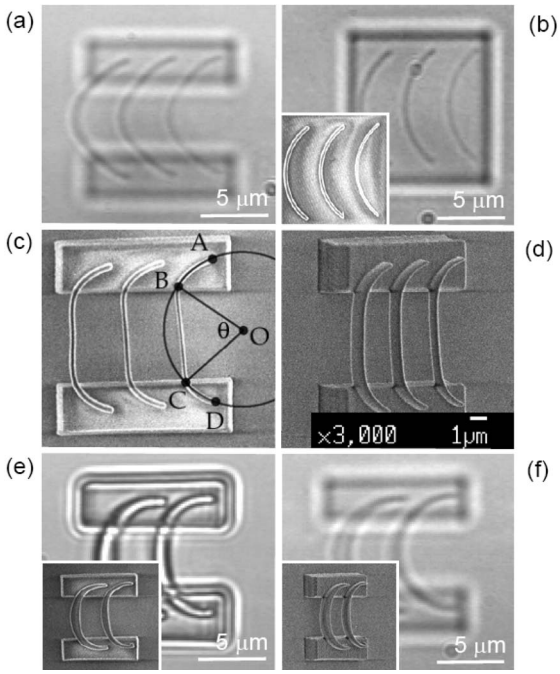

Fig. 3. Axial shrinkage of polymer wires. (a) and (b) Optical microscopic image of the suspended and the reference bent wires, respectively, both before rinsing. The inset is an SEM image of the reference sample. (c) and (d) Top- and tilt-view SEM images of the same wires as those in (a) after rinsing and dried. (e) and (f) Bent wires with larger lateral sizes 0.95 and 1.3 μm, respectively. The insets are the SEM images of the corresponding structures.

example, the three bent wires possessing an identical opening angle $\theta=74°$ and radius $r=4.2$ μm but varied lateral thicknesses $\delta_S=340$, 290, and 210 nm, and vertical thicknesses 1015, 845, and 650 nm, respectively [Figs. 3(c) and 3(d)]. The extra length around 0.5 μm due to the wire curve [arc BC in Fig. 3(c)] is completely "absorbed" and redistributed linearly (line BC). This gives a rate of shrinkage ~12%, apparently not reaching the maximum owing to the limit of the experiment. Since the lateral size reduction was measured the same as those in Fig. 1, the overall volume contraction of the wires is ~62%. If the same rate of shrinkage of 35% is assumed to exist in the wire axis direction, the value rises to 72%, almost half an order greater than those measured from bulk polymer.

The phenomenon of unbending was not found in wires of a large size. Minor deformation was distinguished from a wire with $r=4$ μm, $\theta=77°$, and $\delta_S=950$ nm [Fig. 3(e) and its inset] from magnified SEM images, while no change was observed in the wire of $\delta_S=1.3$ μm [Fig. 3(f)]. With an extension of the rinsing duration to 50 min, both of the wires took their original forms. Here the thickness of the "cleaned" portion is still small compared with the entire wire volume even after sufficient rinsing such that the transparent layer does not affect the properties of the entire wire significantly; the wire wasn't unbent. This result points out that the permeability effect is size related.

Immediate questions related to the concept of the transparent polymer are whether it is a relatively stable state of nanopolymers and what properties that are not seen in bulk materials it provides. Experimentally, we found that when the aforementioned array of wires consisting of dried transparent polymers [Fig. 3(a)] were immersed into the solvent, the wires "remember" their original shape [Fig. 4(a)] and are restored to a bent form as designed [Fig. 4(b)]. More hints on the unique performance of the transparent polymer are found in our previous study on sub-micro-oscillators, where the spring constant of a 300-nm-diameter polymer wire was found to the third-order smaller than that from the calculation [8]. The supersoftness of the spring [8,17] is now interpretable as a natural result of the decreased mechanical strength owing to the polymer permeability.

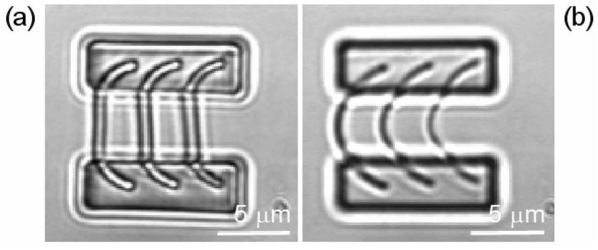

Fig. 4. Shape-memory effect of the wires. (a) Optical microscopic images of the same structures as Fig. 3(c) after rinsing. (b) Same structure after immersing into the solvent of ethanol.

In summary, when the cross-sectional size of femtosecond laser-prototyped polymer wires is sufficiently small, e.g., <1 μm, the polymer network becomes permeable to solvent molecules owing to the removal of the small molecular species involved in the polymerization reaction. The nanopolymers of this status, having a loosened network of polymer chains, are mechanically stable. When wires are dried, an unusually larger volume shrinkage occurs, which is considered to be the origin of super resolution in the two-photon photopolymerization.

The authors would like to acknowledge National Science Foundation of China (NSFC) 60525412 and 60677018, China and the grant-in-aid (A) 17201033, Japan Society for the Promotion of Science, Japan for support.

References

1. C. N. LaFratta, J. T. Fourkas, B. T. Baldacchini, and R. A. Farrer, Angew. Chem. **46**, 6238 (2007).
2. J. J. Li and J. T. Fourkas, Mater. Today **10**, 30 (2007).
3. H.-B. Sun, S. Matsuo, and H. Misawa, Appl. Phys. Lett. **74**, 786 (1999).
4. M. Straub and M. Gu, Opt. Lett. **27**, 1824 (2002).
5. Q.-D. Chen, D. Wu, L.-G. Niu, J. Wang, X.-F. Lin, H. Xia, and H.-B. Sun, Appl. Phys. Lett. **91**, 171105 (2007).
6. S. Yokoyama, T. Nakahama, H. Miki, and S. Mashiko, Appl. Phys. Lett. **82**, 3221 (2003).
7. P. Galajda and P. Ormos, Appl. Phys. Lett. **78**, 249 (2001).
8. H.-B. Sun, K. Takada, and S. Kawata, Appl. Phys. Lett. **79**, 3173 (2001).
9. S. Maruo and H. Inoue, Appl. Phys. Lett. **91**, 084101 (2007).
10. S. R. Marder, J. L. Bredas, and J. W. Perry, MRS Bull. **32**, 561 (2007).
11. A. Xie, T. Ito, and D. A. Higgins, Adv. Funct. Mater. **17**, 1515 (2007).
12. J. Kato, N. Takeyasu, Y. Adachi, H.-B. Sun, and S. Kawata, Appl. Phys. Lett. **86**, 044102 (2004).
13. S. Kawata, H.-B. Sun, T. Tanaka, and K. Takada, Nature **412**, 697 (2001).
14. D. Y. Yang, S. H. Park, T. W. Lim, H. J. Kong, S. W. Yi, H. K. Yang, and K. S. Lee, Appl. Phys. Lett. **90**, 013113 (2007).
15. D. F. Tan, Y. Li, F. J. Qi, H. Yang, Q. H. Gong, X. Z. Dong, and X. M. Duan, Appl. Phys. Lett. **90**, 071106 (2007).
16. H.-B. Sun, T. Tanaka, and S. Kawata, Appl. Phys. Lett. **80**, 3073 (2002).
17. S. Nakanishi, S. Shoji, S. Kawata, and H.-B. Sun, Appl. Phys. Lett. **91**, 063112 (2007).